Electronic Research Archive

ERA, 32(2): 707–732.
DOI: 10.3934/era.2024034
Received: 24 November 2023
Revised: 27 December 2023
Accepted: 29 December 2023
Published: 10 January 2024

http://www.aimspress.com/journal/ERA

Research article

Hybrid short-term traffic flow prediction based on the effect of non-linear sequence noise

Gang Cheng[1,*] and Yadong Liu[2]

[1] College of Engineering, Tibet University, Lhasa 850000, China
[2] College of Information Science and Technology, Tibet University, Lhasa 850000, China

* **Correspondence:** Email: fengyunleng@163.com.

Abstract: Short-term traffic flow prediction is crucial for intelligent transport systems and mitigating traffic congestion. Therefore, precise prediction of real-time traffic conditions is becoming more important. Currently, the existing prediction models lack the ability to effectively extract spatio-temporal characteristics and fail to adequately account for the impact of non-linear noise. To address these issues, the study proposes a hybrid short-term traffic flow prediction model based on spatio-temporal characteristics. First, the method decomposes the initial spatio-temporal traffic sequence data into multiple modal components using the complementary ensemble empirical modal decomposition method. Then, spatio-temporal characteristics are extracted from the decomposed spatio-temporal components using a deep residual network. The predicted values of each factor are combined to obtain the final predicted values. To validate the model, traffic flow data that is collected at point 4909A on the M25 motorway in London is used. The results indicate that the proposed model outperforms other models in terms of accuracy metrics such as root mean square error, mean absolute percentage error, mean absolute error, mean squared error, and coefficient of determination. Therefore, the model has high accuracy and practicality and exhibits great potential for short-term traffic flow prediction.

Keywords: short-term traffic flow prediction; non-linear noise; complementary ensemble empirical modal decomposition; spatio-temporal characteristics; deep residual networks

1. Introduction

With traffic congestion becoming an increasingly serious problem, intelligent transportation systems (ITS) are one of today's most effective approaches to traffic control [1–3]. Short-term traffic flow prediction is important for ITS operations. It involves measuring traffic flow in minutes, hours, and days using historical data analysis, which provides predictive insights to improve traffic guidance efficiency [4]. Short-term traffic flow prediction includes various categories, such as parametric class prediction, shallow machine learning prediction, and deep learning prediction [5].

The autoregressive integrated moving average model (ARIMA) [6] is a parametric classification prediction method. It utilizes mathematical and statistical techniques to analyze historical traffic flow data based on the linear theory of time series. However, due to the unpredictable and unstable nature of traffic flow, ARIMA is unable to address non-routine traffic flow prediction problems.

Prediction based on shallow machine learning involves the utilization of a single layer or a small number of layers in neural network models for prediction tasks, primarily encompassing support vector regression. Model prediction occurs when high-dimensional data is encountered. The processing speed is slow, the computational cost is relatively high, and there is a delay in the output [7].

Deep learning-based prediction utilizes various multi-layer neural networks, including long short-term memory neural networks (LSTM), gated recurrent unit neural networks, and stacked self-encoder neural networks [8,9]. These models learn and train autonomously by processing large amounts of raw data to capture non-linear relationships, although they need sufficient training data and have limited generalization abilities.

With the rise of deep learning, neural networks have been widely used in traffic flow prediction, and their powerful learning ability and adaptive capability have attracted the attention of scholars both at home and abroad. LSTM is a widely used model that is highly accurate, robust, and fault-tolerant for time series problems. However, it only addresses the temporal characteristics of traffic flow data and does not solve the spatial characteristic problem [10]. Researchers have proposed a CNN-LSTM model to address this issue. The model combines a CNN for spatial characteristics extraction and an LSTM for temporal characteristics capture [11]. However, when dealing with extremely long time series, the CNN-LSTM hybrid model's performance may be affected, and it cannot accurately extract spatio-temporal characteristics.

The existing studies are focused on the temporal and spatial characteristics of short-term traffic flow prediction models. However, these studies have mostly neglected the external factors that affect the prediction accuracy of short-term traffic flow. Moreover, these works do not consider the noise interference in traffic flow sequences as well.

In this study, on the basis of focusing on spatio-temporal characteristics. We address the limitations of previous research by considering external factors and reducing the problem of nonlinear noise interference in traffic flow sequences. This significantly improves the accuracy and efficiency of the model, providing a new perspective on short-term traffic flow prediction. In this study, the spatio-temporal characteristics are extracted using deep residual networks with spatio-temporal attention mechanisms (ST-ResNet) based on CNN-LSTM. At the same time, the original traffic flow spatio-temporal sequence data are divided into various modal components using complementary ensemble empirical modal decomposition (CEEMD), and the prediction is carried out for each component. Finally, the prediction values of each component are combined to obtain the final prediction results.

The remainder of this study is organized as follows: Section 2 reviews the relevant literature.

Section 3 details the research methodology and the corresponding model. Section 4 presents the analysis results and validates the model using data. Section 5 summarizes the findings.

2. Literature review

The ITS is a large and complex system with a time-varying nature. An accurate prediction of short-term traffic flow is a crucial element of ITS [12]. Short-term traffic flow prediction is concerned with people's daily travel and traffic operations, specifically on road, rail, air, and water transportation. It predicts future demand by analyzing the historical data and extracting the temporal relationships among various variables [13,14]. Short-term traffic flow prediction can be classified into three categories, namely parameter-based prediction, shallow machine learning-based prediction, and deep learning-based prediction [5]. Saleh et al. utilized an ARIMA model based on linear time series theory for performing predictions. However, the results were unsatisfactory due to the challenge of capturing the spatial and temporal correlations in traffic flow time series without considering the spatial factors in the ARIMA [15]. Huang et al. used support vector machines for traffic flow prediction, which reduce the computation time effectively when the data size is large, but the model may get stuck in the local optima [16]. The recurrent neural networks (RNNs) are very good for time series modeling and prediction, but the RNNs suffer from gradient exploding and gradient vanishing problems [17]. Because of their unique operational mode, training these models is a challenging task.

Duan et al. proposed the use of self-automated encoders to represent the traffic flow features for performing predictions based on deep neural networks. This approach identified the non-linear spatio-temporally correlated traffic flow characteristics of traffic data [18]. In order to address the gradient explosion of RNNs, Ma et al. initially employed an LSTM model for predicting the traffic speed on urban arterial roads [19]. The LSTM learn time series with long-term dependencies without specifying a time extension. Hussain et al. utilized a GRU network for short-term traffic flow prediction. They also proposed a combined analysis of hyper-parameter optimization and window step adjustment for time series prediction [20] Jiang et al. conducted a review of GNN traffic flow prediction models and observed that the GNN effectively handles the spatio-temporal relationships between traffic flow sequences. Additionally, when combined with other advanced techniques, GNN achieves higher prediction accuracy [21]. Li et al. used a convolutional neural network (CNN) and an LSTM consisting of a CNN-LSTM model to predict the traffic flow in the next 24 hours [22]. Dai et al. used a GRU model combined with spatio-temporal characteristics for passenger flow prediction. The results indicate that this combined model is more accurate and stable compared to the standalone GRU model [23]. Zhang et al. proposed DeepST, a CNN-based urban flow prediction model [24]. The flow of people was categorized into three modules: closure, periodicity, and trend. He et al. proposed deep residual learning to predict the flow of people in urban railways. They addressed the issues of gradient explosion and gradient vanishing by incorporating "residual connections". The effectiveness of the model has been demonstrated in experiments [25]. Zhang et al. proposed the ST-ResNet model, which employs the residual network architecture to improve the spatio-temporal modeling ability of the system, and it has been demonstrated to outperform DeepST [26]. Wu et al. proposed integrated empirical mode decomposition (EEMD), which is an auxiliary method for noise analysis. EEMD automatically eliminates the existence of mode mixing problem by adding white noise in the signal subject to analysis [27]. However, choosing appropriate white noise amplitude and determining the number of integration experiments should be further investigated. Huang et al. used complementary

ensemble empirical mode decomposition (CEEMD) to address the mode mixing phenomenon of EMD. CEEMD has a higher accuracy and is more computationally efficient [28]. Table 1 shows recent research literature related to short-term traffic flow.

Table 1. Research on short-term traffic flow prediction model.

Author	Title	Main characteristics & results
Lou et al. [29]	Attention-based gated recurrent graph convolutional network for short-term traffic flow prediction	The model introduces an attentional mechanism to adaptively learn the relationship between different time steps. However, it does not take into account the effects of external factors and noise.
Li et al. [30]	A dynamic spatio-temporal deep learning model for lane-level traffic prediction	The model uses GCN to capture spatio-temporal features. However, it considers too few features factors and does not take into account traffic flow noise for poor applicability.
Yang et al. [31]	Short-term traffic flow prediction based on AST-MTL-CNN-GRU	The model proposed in the article improves the stability and accuracy of model predictions, yet ignores the effects of external factors and noise.
Zhao et al. [32]	Short-term traffic flow prediction based on VMD and IDBO-LSTM	This study addresses noise generated by short-term non-linear traffic flows. However, it does not consider interference from external factors.
Zhao et al. [33]	Interval short-term traffic flow prediction method based on CEEMDAN-SE noise reduction and LSTM optimized by GWO	The issue of noise effects in non-linear sequences is addressed using CEEMDAN-SE, without considering the effects of external factors.
Jiang X. [34]	A combined monthly precipitation prediction method based on CEEMD and improved LSTM	Combined with CEEMD, the sequence noise is decomposed and removed. However, the interference of external factors is considered.

The above literature primarily examines the temporal and spatial features of short-term traffic flow data in order to enhance the validity and accuracy of the models. However, these models rarely consider the spatio-temporal features, external factors, and non-linear sequence noise that interferes with the prediction of traffic flow sequences, simultaneously. In this study, the limitations of the existing methods are overcome by proposing a unique hybrid prediction model that simultaneously addresses the interference of all three.

This study utilizes CEEMD to decompose the traffic flow data into eigenmode functions and residual terms. The spatio-temporal features are then extracted using ST-ResNet as well as CNN-LSTM modules. This enables the extraction of temporal and spatial characteristics from the traffic flow data, while allowing us to address the impact of external factors, such as holidays and weather, etc., as well as the effect of non-linear noise on short-term traffic flow sequences. Through experimental validation, this study successfully addresses the issue of reduced accuracy in short-time

traffic flow prediction caused by external factors and non-linear noise. It also improves the applicability and accuracy of the model.

3. Methodology

In this section, a hybrid CEEMD-ST-ResNet-CNN-LSTM model for short-term traffic flow prediction is presented. The proposed model aims to address the issue of degraded prediction accuracy due to exogenous factors and non-linear disturbances. The proposed model first decomposes the traffic flow data into smooth modal and residual components using the CEEMD method. It then extracts the spatio-temporal characteristics of each component using the ST-ResNet-CNN-LSTM model. Finally, all the prediction components are integrated to obtain the final results.

The main steps are presented below.

Step 1: Data processing

Data normalization: In order to restrict the output to [-1,1] [35], data normalization is applied to the output of the tanh function in ST-ResNet. The equation for normalization is:

$$x_{normalized} = \frac{\left(x - x_{\min}\right)}{\left(x_{\max} - x_{\min}\right)} \tag{1}$$

where, x denotes the original value of traffic flow data, $x_{\min}$ denotes the minimum value of traffic flow data, and $x_{\max}$ denotes the maximum value of traffic flow data.

Step 2: Non-linear sequence noise processing

Step 2.1: CEEMD is capable of decomposing non-linear and non-stationary signals into a set of modal functions, effectively extracting both the primary signal components and the noise components. This study utilizes CEEMD to decompose the data. It adds n sets of positive and negative pairs of auxiliary white noises in the original traffic flow sequences. This results in a set containing 2n signals [36].

$$\begin{bmatrix} M1 \\ M2 \end{bmatrix} = \begin{bmatrix} 1 & 1 \\ 1 & -1 \end{bmatrix} \begin{bmatrix} S \\ N \end{bmatrix} \tag{2}$$

where, S represents the original signal of the traffic flow sequence, N is the auxiliary white noise, and $M1$ and $M2$ are the signals after adding positive and negative paired white noise, respectively.

Step 2.2: CEEMD decomposition is performed for each sequence signal in the set, and a set of IMF components is obtained for each sequence signal, where the j-th IMF component of the i-th component is denoted as c_{ij}.

Step 2.3: Multi-component quantities are averaged to obtain the decomposition results.

$$c_j = \frac{1}{2}\sum_{i=1}^{2n} c_{ij} \tag{3}$$

where, c_j represents the j-th IMF component that is finally obtained after decomposition.

Step 3: Extract the spatio-temporal characteristics of the traffic flow sequence.

Step 3.1: In this study, the IMF signal after CEEMD decomposition is used as the input of CNN for extracting the spatio-temporal characteristics from the traffic flow data. The convolutional layers of CNN extract the local characteristics by connecting upper layers through each neuron. The pooling layer further extracts the characteristics based on the convolutional layer, preventing overfitting in spatial characteristic extraction of traffic flow sequences [37,38]. The convolution operation (4) and

pooling operation (5) are described below:

$$x_j^l = conv\left(\sum x_j^{l-1} \times w_{i,j}^l + b_j^l\right) \tag{4}$$

where, x_j^{l-1} and x_j^l are the inputs and outputs, respectively (l is the length of the traffic flow sequence, i and j denote the processing positions in the convolution process), $w_{i,j}^l$ is the weight of the convolutional layer, and b_j^l is the bias of the convolution layer.

$$x_j^{l+1} = pooling\left(x_j^l\right) \tag{5}$$

The pooling function represents the pooling operation, and x_j^{l+1} denotes the output after the pooling layer.

Step 3.2: The CNN initially extracts the spatial characteristic vectors from the traffic flow sequence, which are then used as the input of the LSTM model for preliminary temporal characteristic extraction. LSTM achieves information inflow and direct state updating through the introduction of input gates, output gates, and forgetting gates. Based on "gates", it effectively solves the problem of accuracy degradation due to the gradient explosion and gradient disappearance during the prediction of traffic flow [39,40]. LSTM extracts the temporal features of traffic flow as follows [41]: First, the information is calculated by the sigmoid function, as shown in (6) and (7).

$$\delta(x) = \frac{1}{1+\exp(-x)} \tag{6}$$

$$i_t = \delta\left(W_i \times \left[h_{t-1}, x_t\right] + b_i\right) \tag{7}$$

where, $\delta(x)$ denotes the sigmoid function, i_t represents the output of the input gate at moment t, δ represents the sigmoid activation function, W_i is the weight of the input gate, h_{t-1} is the input of the network at the previous moment, x_t denotes the input of the current network, and b_i denotes the bias of the input gate.

Then, the amount of information stored in the cell state is updated as determined by an input gate. The memory cell and input gate output equations are shown in (8) and (9). Afterward, by merging the forgetting gate with the input gate, the updated cell state is calculated, as shown in (10).

$$f_t = \delta\left(W_f \times \left[h_{t\text{-}1}, x_t\right] + b_f\right) \tag{8}$$

$$C_{t1} = \tanh\left(W_C \times \left[h_{t-1}, x_t\right] + b_C\right) \tag{9}$$

$$C_t = f_t \times C_{t-1} + i_t \times C_{t1} \tag{10}$$

where, f_t denotes the output of the forgetting gate, W_f is the weight of the forgetting gate, b_f denotes the bias of the forgetting gate, C_{t1} denotes the output of the memory cell, W_C represents the weight of the output gate, b_c is the bias of the output gate, C_t denotes the output of the memory cell, and C_{t-1} represents the state of the previous memory cell.

Finally, the outputs are computed using the updated cell states. The outputs from the tanh compression and sigmoid gates are multiplied together to obtain the predicted traffic flow sequence. The tanh activation function is shown in (11), and the outputs are presented in (12) and (13).

$$\tanh(x) = \frac{\exp(x) - \exp(-x)}{\exp(x) + \exp(-x)} \tag{11}$$

$$o_t = \delta\left(W_o \times \left[h_{t-1}, x_t\right] + b_o\right) \tag{12}$$

$$h_t = o_t \times \tanh(c_t) \tag{13}$$

where, o_t denotes the output of the output gate at moment t, W_o represents the weight of the computing unit, b_o denotes the bias of the computing unit, and h_t denotes the predicted traffic flow sequence.

Step 3.3: This study inputs the extracted traffic flow temporal characteristic vectors from LSTM, and the initially extracted spatial characteristics from CNN into the ST-ResNet model for further extraction of spatio-temporal characteristics. This model has four components, including temporal proximity, period, trend, and external influence [42]. This study divides the timeline into three segments, and each segment is used in the first three components to deal with closeness, trend, and periodicity [26]. All three modules utilize an identical network for extracting the spatio-temporal characteristics. This network comprises forward and backward convolutional networks as well as residual units. The external module of ST-ResNet inputs external factors, such as holiday information and weather data, into two fully connected layers. It then combines the outputs of the three components as X_{Res}, such that the parameter matrix assigns different weights to the results of different components in different regions. X_{Res} with the output further integrates the external components X_{Ext} and obtains the final predicted values X_t [43].

Step 3.4: Inverse normalization is performed on the data to restore the traffic flow information to its original range, enabling easier model evaluation. The inverse normalization is mathematically expressed as follows [44]:

$$x_{normalized} = x_{original} \times (x_{\max} - x_{\min}) - x_{\min} \tag{14}$$

where, $x_{normalized}$ is the normalized traffic flow data, $x_{\min}$ is the minimum value of the original data, and $x_{\max}$ is the maximum value of the original data.

Step 4: Model performance evaluation

Step 4.1: In order to evaluate the predictions of the model, this work uses several metrics, including root mean square error (RMSE), mean absolute percentage error (MAPE), mean absolute error (MAE), mean square error (MSE), and the coefficient of determination R^2. These metrics are used to measure the prediction accuracy. As errors increase, so does the prediction error, and vice versa. The range of R^2 is [0, 1], with higher values indicating greater accuracy. In general, more than 80% meets the prediction requirements, and more than 90% exhibits strong prediction capabilities [45,46]. The metrics are mathematically defined as follows:

$$RMSE = \sqrt{\frac{1}{N}\sum_{i=1}^{N}(y_i - \hat{y}_i)^2} \tag{15}$$

$$MAPE = \frac{100\%}{n}\sum_{i=1}^{n}\left|\frac{\hat{y}_i - y_i}{y_i}\right| \tag{16}$$

$$MAE = \frac{1}{n}\sum_{i=1}^{n}|\hat{y}_i - y_i| \tag{17}$$

$$MSE = \frac{1}{n}\sum_{i=1}^{n}(y_i - \hat{y}_i)^2 \tag{18}$$

$$R^2 = 1 - \frac{\sum_i\left(\hat{y}_i - y_i\right)}{\sum_i\left(\overline{y_i} - y_i\right)} \tag{19}$$

where, y_i represents the predicted value at moment *i*, y_i denotes the true value at moment *i*, and $\overline{y_i}$ represents the mean value at moment *i*. RMSE is used to measure the stability of the result. MAPE, MAE, and MSE are used to measure the error of the prediction result, and R^2 is used to measure the accuracy of the prediction results.

4. Experimental simulation

4.1. Data sources

The primary data sources used in this study include the publicly available data from the M25 motorway, London (http://tris.highwaysengland.co.uk/detail/trafficflowdata) and the publicly available meteorological data from the UK Meteorological Office. The data used in this work spans from September 6 to September 7, 2019, with recordings captured every 15 minutes, resulting in a total of 1200 data points. The four weather types include temperature ranging between [13, 21] ℃, wind speed ranging between [1, 7.9] m/s, and average vehicle speed ranging between [24.82, 109.83] km/h. The dataset is split into three sets, including training, validation, and test sets, with a ratio of 8:1:1. In order to prevent overfitting, the training set is used as an evaluation criterion.

4.2. Parameter setting

The model was developed using MATLAB 2022a. The CNN's convolutional layer has a size of 2 × 1 and ten channels. The pooling layer window size is 2 × 1 with a step size of 1. The residual connection block has four 1 × 1 convolutional layers, and the model was trained using the Adam optimizer.In order to obtain the optimal parameters, manual parameter tuning is performed by repeating the experiments. The optimal parameter configurations are presented in Table 2. The results of parameter comparisons are presented in Tables 3–11. The remaining parameters are subject to sensitivity analysis discussed in Section 4.2.

Table 2. The optimal parameter setting.

Parameter name	Parameter value
Number of max modal decomposition	6
Hidden size	32
Learning rate	0.004
Batch size	12
Number of filters	58

Table 3. The hidden size predictive indicators (during training).

Hidden size	RMSE	MAPE	MAE	MSE	R^2
30	4.0683	0.096702	3.1324	16.5511	0.99492
31	3.8493	0.096483	10.9841	14.8168	0.99545
32	1.5947	0.040587	1.1793	2.5431	0.99922
33	4.3437	0.11937	2.6458	18.8673	0.99421
34	4.0008	0.07027	2.1736	16.0063	0.99509

Table 4. The hidden size predictive indicators (during validation).

Hidden size	RMSE	MAPE	MAE	MSE	R^2
30	18.7609	0.10459	13.8687	351.9706	-1.0403
31	12.4847	0.087168	10.9841	155.8678	0.096483
32	12.9028	0.089886	10.9997	166.4817	0.034958
33	16.9168	0.10315	12.5902	286.1783	-0.65889
34	12.3519	0.089147	11.0359	152.5686	0.11561

Table 5. The hidden size predictive indicators (during test).

Hidden size	RMSE	MAPE	MAE	MSE	R^2
30	29.4357	0.70872	24.3286	866.4614	-0.2577
31	32.4105	0.79179	29.5891	1050.4407	-0.52475
32	26.1248	0.64509	22.4533	682.5035	0.0093219
33	39.5779	0.89554	35.9724	1566.4081	-1.2737
34	37.2305	0.91889	33.5371	1386.112	-1.012

Table 6. The learning rate predictive indicators (during training).

Learning rate	RMSE	MAPE	MAE	MSE	R^2
0.002	1.7499	0.057602	1.36	3.062	0.99906
0.003	1.9276	0.060317	1.4096	3.7156	0.99886
0.004	1.5947	0.040587	1.1793	2.5431	0.99922
0.005	1.5999	0.045694	1.2485	2.5596	0.99921
0.006	1.7446	0.043963	1.2747	3.0436	0.99907

Table 7. The learning rate predictive indicators (during validation).

Learning rate	RMSE	MAPE	MAE	MSE	R^2
0.002	17.7756	0.10622	13.691	315.9719	-0.83159
0.003	10.6766	0.075597	9.0665	113.9901	0.33924
0.004	12.9028	0.089886	10.9997	166.4817	0.034958
0.005	14.4383	0.093439	11.7949	208.4649	-0.20841
0.006	11.8831	0.075512	9.2744	141.2076	0.18146

Table 8. The learning rate predictive indicators (during test).

Learning rate	RMSE	MAPE	MAE	MSE	R^2
0.002	21.926	0.53422	18.7745	480.7515	0.30217
0.003	23.9992	0.5933	21.6786	575.9625	0.16397
0.004	26.1248	0.64509	22.4533	682.5035	0.0093219
0.005	25.3748	0.63345	22.1973	643.878	0.065388
0.006	31.2697	0.74815	27.3052	977.7969	-0.41931

Table 9. The batch size predictive indicators (during training).

Batch size	RMSE	MAPE	MAE	MSE	R^2
10	2.2853	0.065039	1.6792	5.2224	0.9984
11	3.7803	0.078748	2.5268	14.2908	0.99561
12	1.5947	0.040587	1.1793	2.5431	0.99922
13	3.6089	0.10178	2.5309	13.024	0.996
14	2.2327	0.048726	1.5572	4.9851	0.99847

Table 10. The batch size predictive indicators (during validation).

Batch size	RMSE	MAPE	MAE	MSE	R^2
10	12.8564	0.086228	10.8732	165.287	0.041883
11	15.0551	0.11038	13.5224	226.6549	-0.31385
12	12.9028	0.089886	10.9997	166.4817	0.034958
13	13.2761	0.89554	9.961	176.2559	-0.0217
14	12.1953	0.084192	10.3098	148.7253	0.13789

Table 11. The batch size predictive indicators (during test).

Batch size	RMSE	MAPE	MAE	MSE	R^2
10	23.2552	0.5348	19.9499	540.8049	0.215
11	22.3152	0.55195	19.3492	497.9666	0.27718
12	26.1248	0.64509	22.4533	682.5035	0.0093219
13	24.8586	0.57737	23.1957	617.9524	0.10302
14	29.2943	0.73724	26.6039	858.1544	-0.24564

4.3. Model sensitivity analysis

In this study, we investigate the impact of the number of filters in the deep spatio-temporal residual block (ST-ResNet), the maximum number of modal decompositions of CEEMD, hidden size, learning rate, and batch size on the performance of the model. The prediction model is evaluated using RMSE, MSE, MAPE, MAE, and R^2.

1) As shown in Tables 12–14, by modifying the number of filters in the deep residual connection block, we observe that the model's prediction accuracy reaches its highest level at 58 filters. Changing the number of filters affects model accuracy. Thus, selecting the right number of filters is crucial for optimal performance in practical applications. The comparative prediction results are presented in Figure 1.

Table 12. The performance analysis based on the number of deep spatio-temporal residual connection filters (during training).

Number of filters	RMSE	MAPE	MAE	MSE	R^2
48	2.3388	0.079259	1.5398	5.4701	0.99832
50	4.9904	0.076096	2.3931	24.9036	0.99236
58	1.5947	0.040587	1.1793	2.5596	0.99922
60	3.8112	0.12705	2.6154	14.5251	0.99554
68	2.3712	0.059729	1.7293	5.6227	0.99827

Table 13. The performance analysis based on the number of deep spatio-temporal residual connection filters (during validation).

Number of filters	RMSE	MAPE	MAE	MSE	R^2
48	13.0967	0.078711	10.0959	171.5231	0.0057344
50	12.5273	0.08717	12.5273	156.934	0.090303
58	12.9028	0.089886	10.9997	166.4817	0.034958
60	12.1918	0.086549	10.2898	148.6398	0.13838
68	14.1821	0.10031	12.195	201.1311	-0.16589

Table 14. The performance analysis based on the number of deep spatio-temporal residual connection filters (during test).

Number of filters	RMSE	MAPE	MAE	MSE	R^2
48	40.0163	0.97274	37.311	1601.3011	-1.3243
50	25.5793	0.64199	22.9982	654.3031	0.050256
58	26.1248	0.64509	22.4533	682.5035	0.0093219
60	32.5832	0.79561	29.6234	1061.6676	-0.54105
68	40.1323	0.96196	38.541	1610.6047	-1.3378

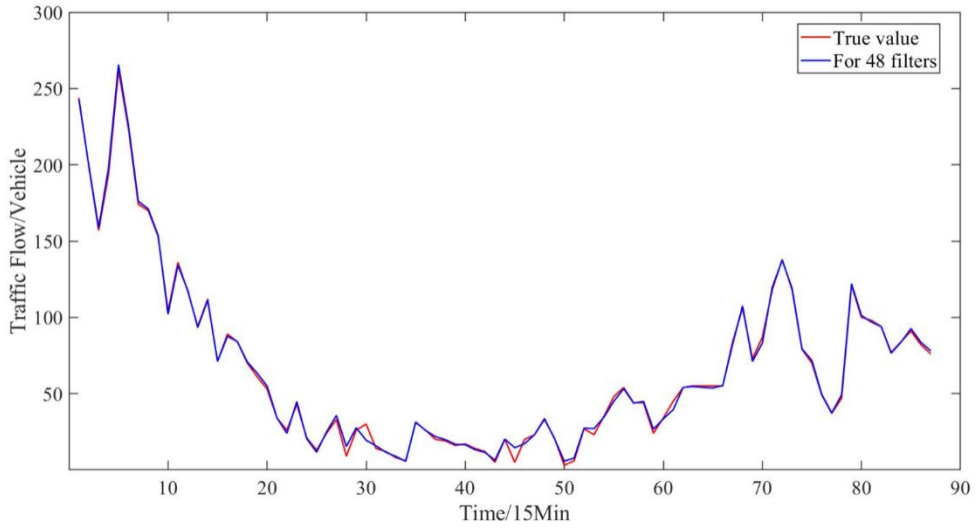

(a)

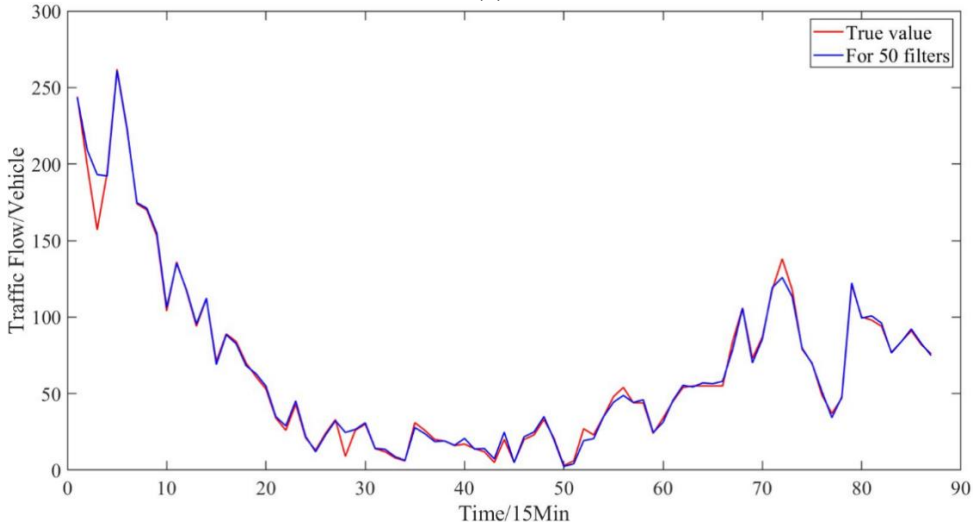

(b)

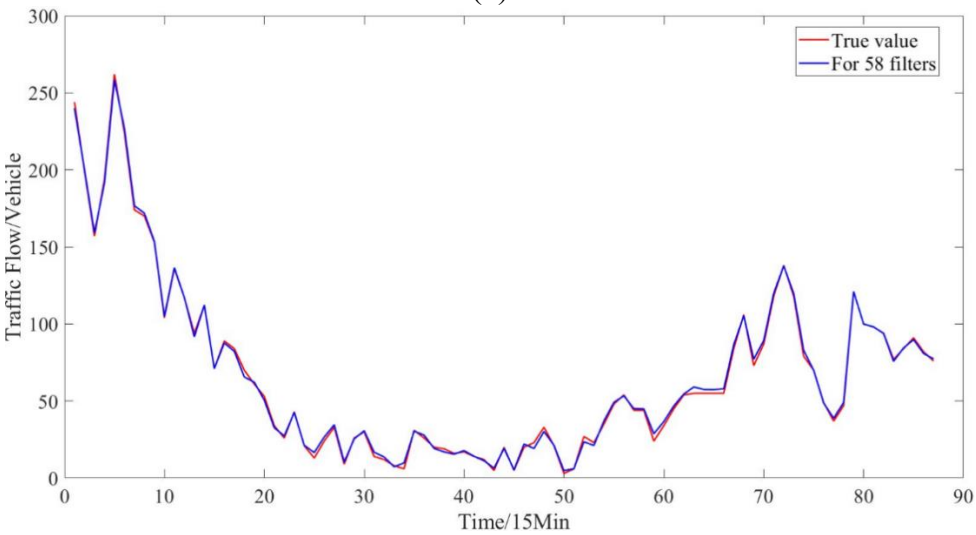

(c)

continued on next page

Figure 1. A performance comparison chart for number of filters. (a) For 48 filters; (b) For 50 filters; (c) For 58 filters; (d) For 60 filters; (e) For 68 filters.

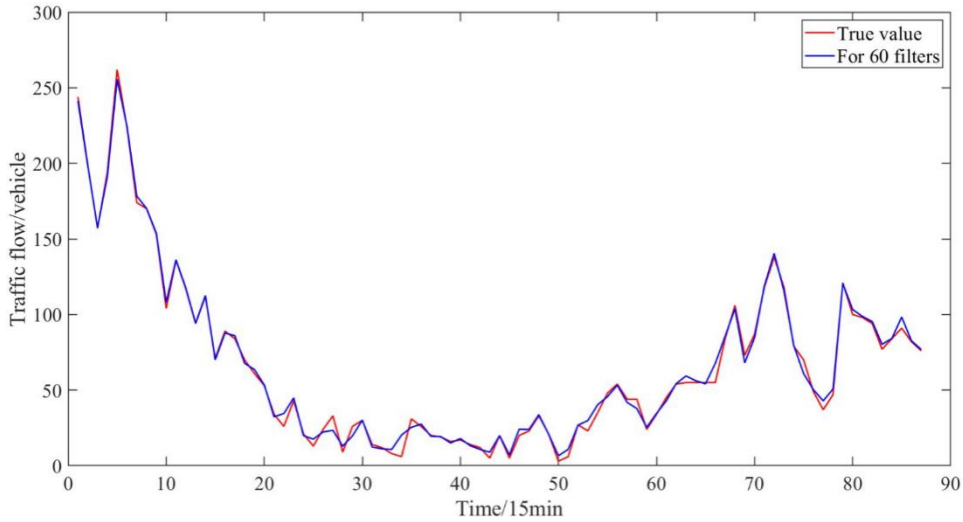

(d)

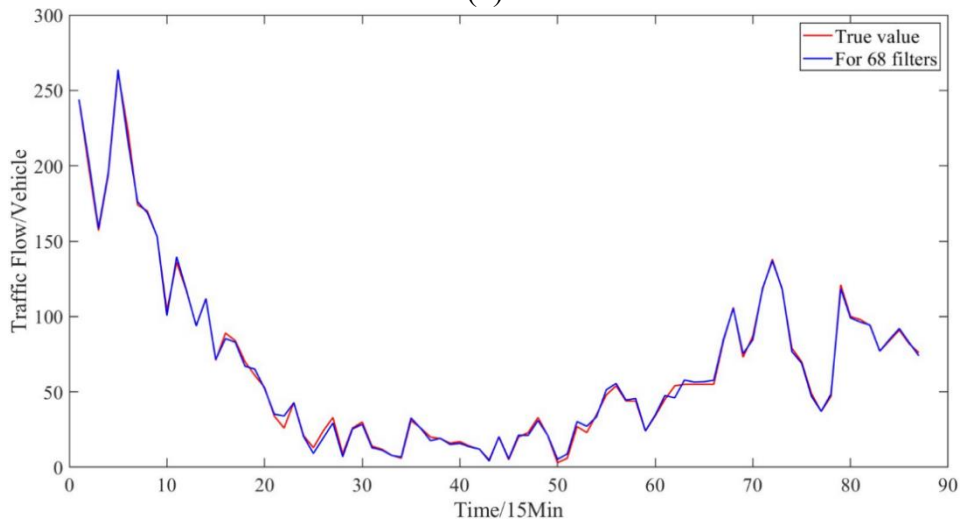

(e)

Figure 1. A performance comparison chart for number of filters. (a) For 48 filters; (b) For 50 filters; (c) For 58 filters; (d) For 60 filters; (e) For 68 filters.

2) In Tables 15–17, when evaluating the sensitivity of the maximum number of modal decompositions in CEEMD, it is observed that the best prediction accuracy is achieved when the maximum number of modal decompositions is set to six. This is due to a decrease in accuracy when the maximum modal decompositions are below six, which may be attributed to the model's inability to sufficiently capture the complexity of the data. When the maximum number of modal decompositions exceeds six, the accuracy of the model decreases, possibly because of redundant information induced by excessive modal decompositions. A performance comparison based on the maximum number of modal decompositions is presented in Figure 2. Based on sensitivity analysis, we can find the optimal parameter configuration to improve the model's predictive accuracy. This guide is crucial for further optimizing and improving the prediction model.

Table 15. The performance analysis based on maximum modal decompositions (during training).

Max modal decomposition number	RMSE	MAPE	MAE	MSE	R^2
3	2.0434	0.049235	1.4847	4.1753	0.99872
4	1.8176	0.0554	1.3952	3.3038	0.99899
5	1.7382	0.040511	1.2721	3.0213	0.99907
6	1.5947	0.040587	1.1793	2.5596	0.99922
7	2.0107	0.047844	1.4778	4.043	0.99876

Table 16. The performance analysis based on maximum modal decompositions (during validation).

Max modal decomposition number	RMSE	MAPE	MAE	MSE	R^2
3	12.8421	0.088619	10.881	164.92	0.044011
4	12.4354	0.085262	10.3728	154.639	0.10361
5	11.9177	0.080739	9.7854	142.0312	0.17669
6	12.9028	0.089886	10.9997	166.4817	0.034958
7	12.3835	0.085008	10.3275	153.3514	0.11107

Table 17. The performance analysis based on maximum modal decompositions (during test).

Max modal decomposition number	RMSE	MAPE	MAE	MSE	R^2
3	37.4849	0.87249	32.9683	1405.1171	-1.0396
4	25.869	0.62776	22.6031	669.2049	0.028625
5	25.1724	0.61301	21.9644	633.6476	0.080238
6	26.1248	0.64509	22.4533	682.5035	0.0093219
7	28.3631	0.70647	24.7633	804.4659	-0.16771

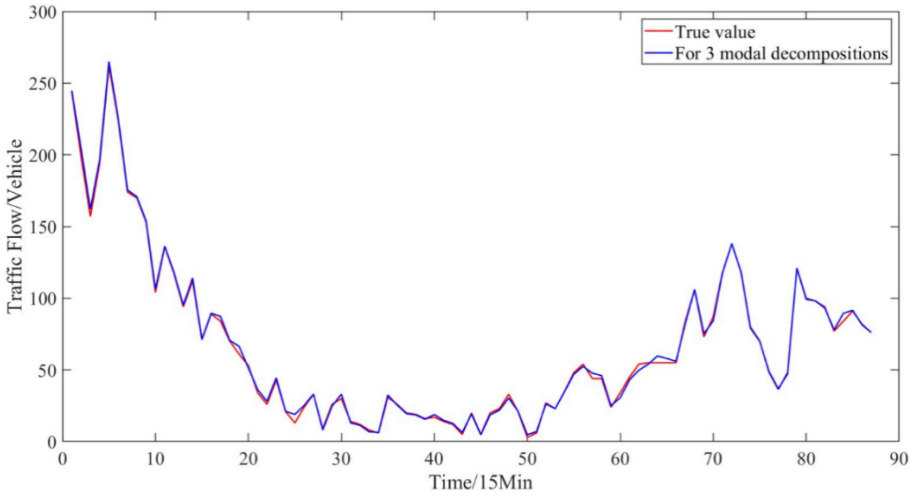

(a)

continued on next page

Figure 2. A performance comparison based on the maximum number of modal decompositions. (a) For three modal decompositions; (b) For four modal decompositions; (c) For five modal decompositions; (d) For six modal decompositions; (e) For seven modal decompositions.

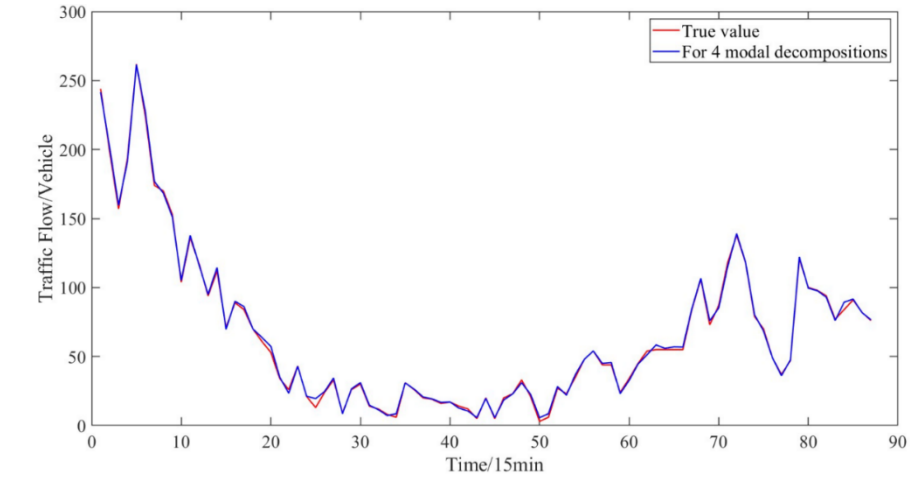

(b)

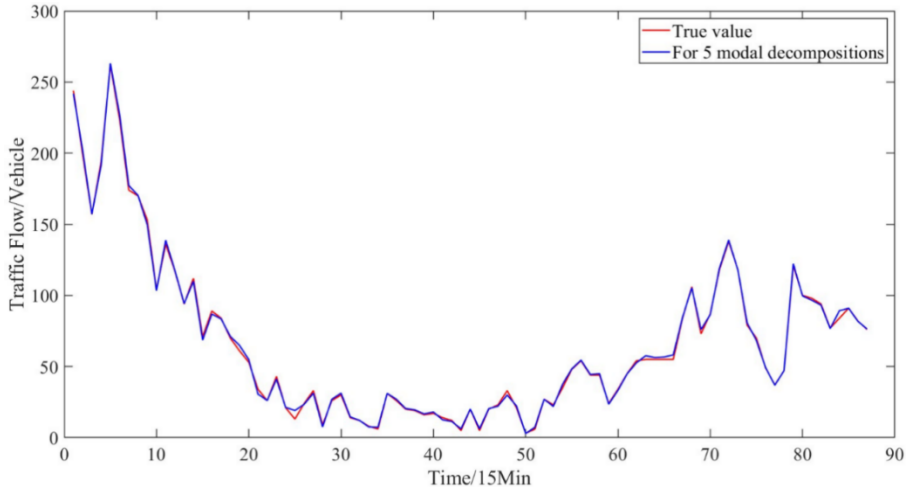

(c)

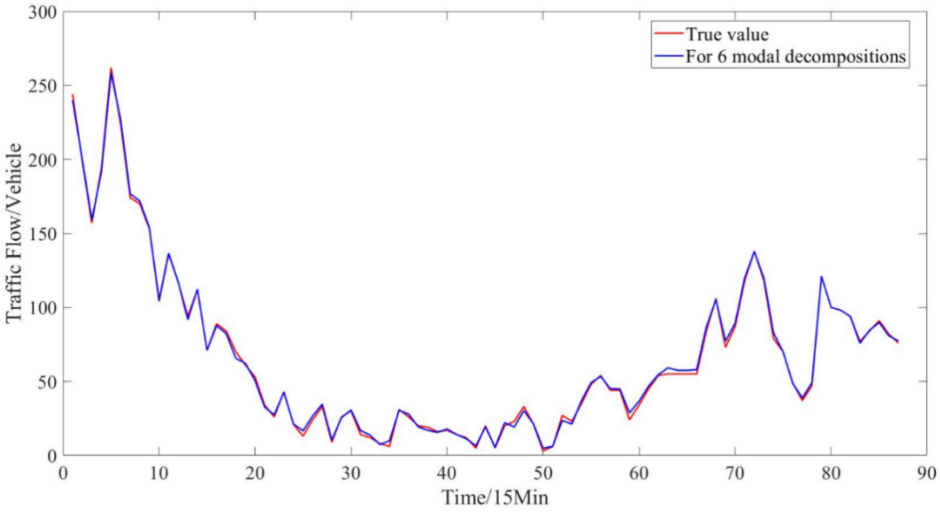

(d)

continued on next page

Figure 2. A performance comparison based on the maximum number of modal decompositions. (a) For three modal decompositions; (b) For four modal decompositions; (c) For five modal decompositions; (d) For six modal decompositions; (e) For seven modal decompositions.

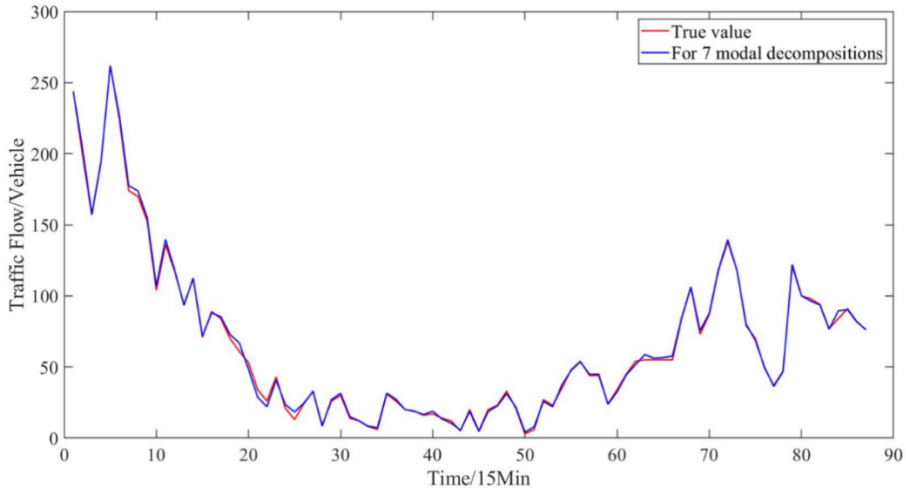

(e)

Figure 2. A performance comparison based on the maximum number of modal decompositions. (a) For three modal decompositions; (b) For four modal decompositions; (c) For five modal decompositions; (d) For six modal decompositions; (e) For seven modal decompositions.

4.4. Model performance evaluation

This study evaluates the model's predictive abilities by comparing its performance with five commonly used benchmark models in short-term traffic flow prediction. This study involves high-dimensional massive data and a variety of dynamic information including holidays and weather, with spatial dependence and time dependence, ARIMA model, which is a traditional linear time series model, cannot deal with this kind of spatio-temporal prediction, and it is not meaningful as a comparison model, so it is not used in this study.The predicted curves are shown in Figure 3, while the CEEMD modal decomposition is shown in Figure 4.

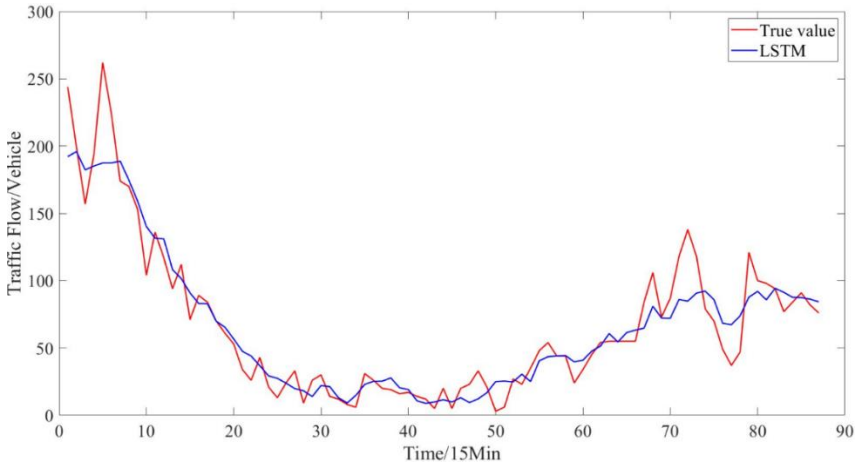

(a)

continued on next page

Figure 3. A comparison chart of performance evaluation; (a) LSTM-based prediction; (b) GRU-based prediction; (c) SVM-based prediction; (d) CNN-based prediction; (e) CNN-LSTM-based prediction; (f) CEEMD-ST-ResNet-CNN-LSTM-based prediction.

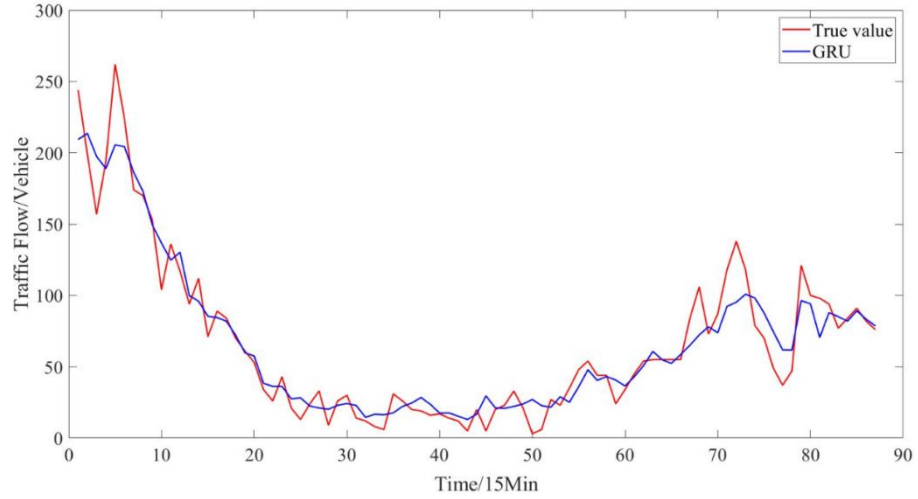

(b)

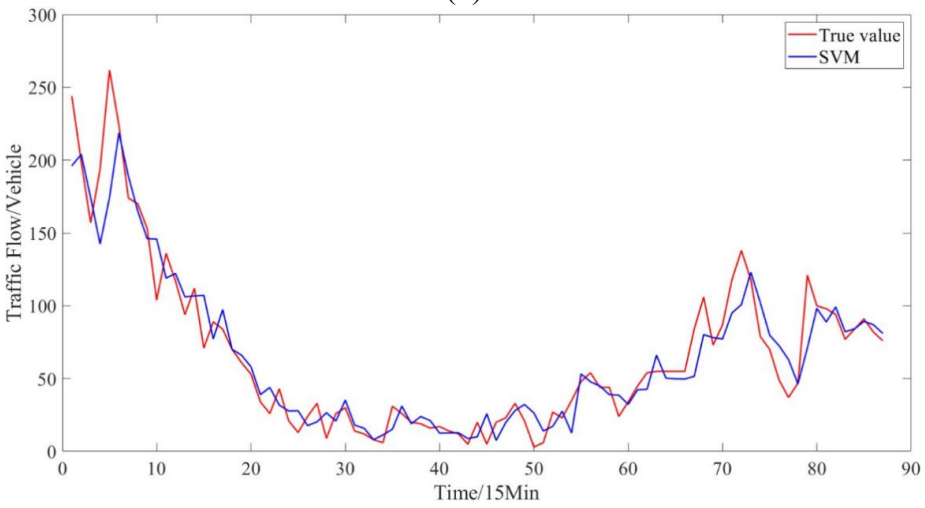

(c)

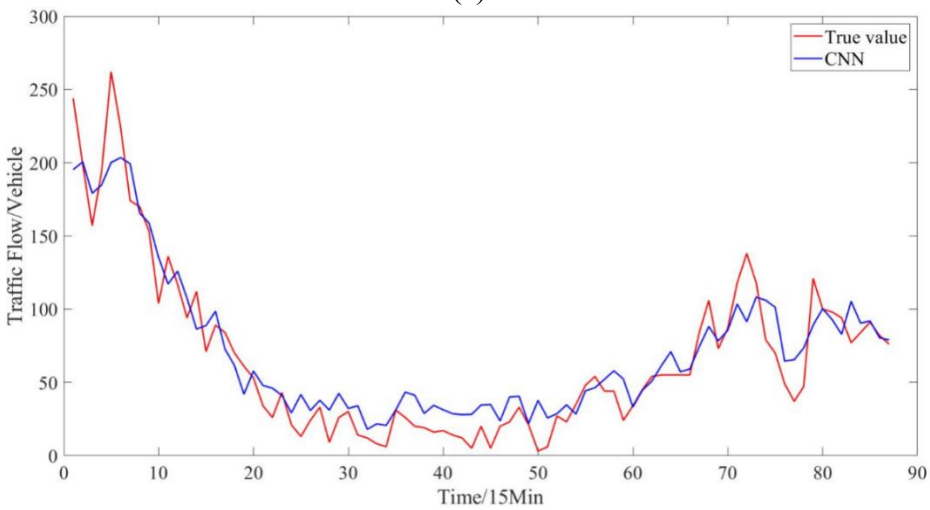

(d)

continued on next page

Figure 3. A comparison chart of performance evaluation; (a) LSTM-based prediction; (b) GRU-based prediction; (c) SVM-based prediction; (d) CNN-based prediction; (e) CNN-LSTM-based prediction; (f) CEEMD-ST-ResNet-CNN-LSTM-based prediction.

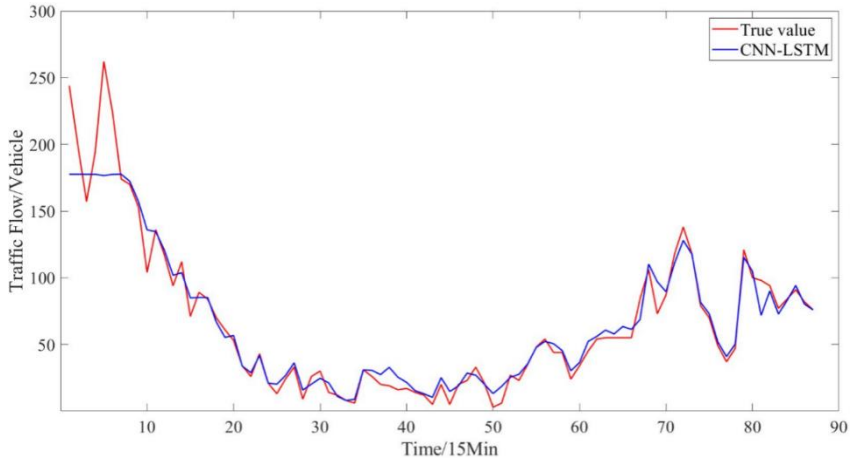

(e)

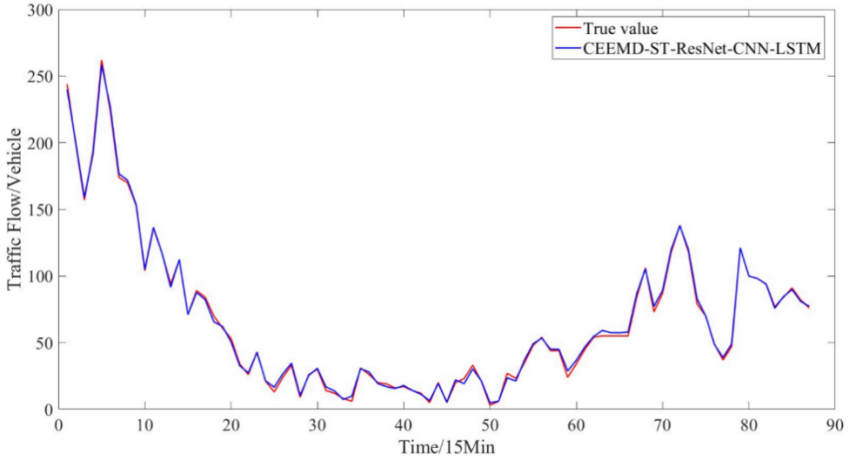

(f)

Figure 3. A comparison chart of performance evaluation; (a) LSTM-based prediction; (b) GRU-based prediction; (c) SVM-based prediction; (d) CNN-based prediction; (e) CNN-LSTM-based prediction; (f) CEEMD-ST-ResNet-CNN-LSTM-based prediction.

LSTM: Demonstrates excellence in time-series data handling, capturing long-term dependencies in traffic flow, and managing data with various time scales, such as hourly and minute-level traffic flow.

GRU: Comparable to LSTM in short-term traffic flow prediction, it is effective in predicting time-series data because of its simplified gating mechanism and has better computational efficiency as compared to LSTM.

SVM: Used for constructing a non-linear regression model for traffic flow prediction, it handles high-dimensional data and is appropriate for predicting traffic flow with multiple characteristics.

CNN: CNN has exceptional spatial feature extraction abilities and can capture spatio-temporal traffic flow relationships. Parameter sharing and local connectivity are advantageous for handling large amounts of data and high dimensionality when predicting traffic flow.

CNN-LSTM: In CNN-LSTM, several convolutional layers and LSTM layers are utilized to extract features of various scales, aiding in the capture of temporal and spatial characteristics for enhanced and precise traffic flow prediction.

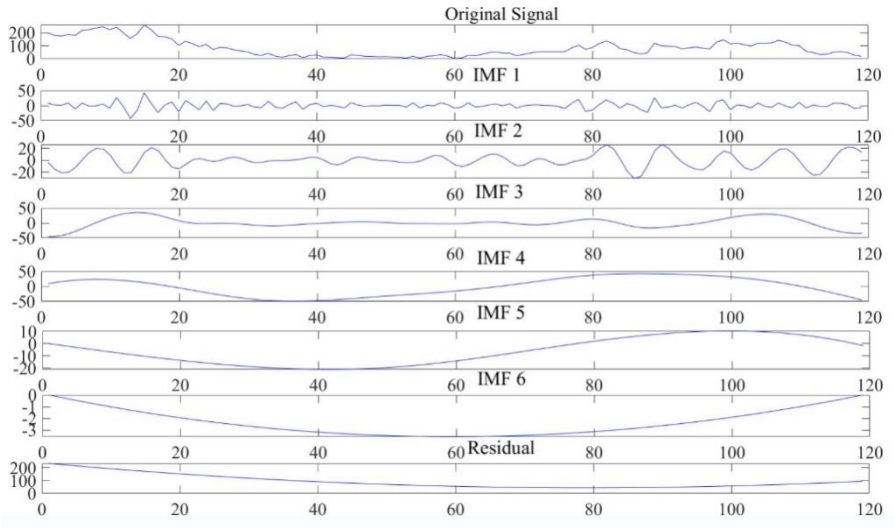

Figure 4. The modal decomposition of CEEMD-ST-ResNet-CNN-LSTM.

Tables 18–20 presents the prediction accuracy of both the proposed model and other benchmark models. The proposed model decreases RMSE by 54.02%, MAPE by 45.74%, MAE by 43.95%, and MSE by 78.72%, outperforming various benchmark models. In addition, the proposed model achieves an accuracy of 99.92%. Therefore, the proposed model exhibits exceptional predictive capability and outperforms alternative benchmark models in terms of all metrics.

Table 18. The performance comparison of different models (during training).

Model	RMSE	MAPE	MAE	MSE	R^2
LSTM	9.6089	0.17426	4.9747	92.3309	0.97166
GRU	7.3905	0.18163	4.3908	54.6202	0.98324
SVM	18.5606	0.39506	12.2087	344.4966	0.89427
CNN	11.9297	0.40695	9.2435	142.3172	0.95632
CNN-LSTM	3.4689	0.074801	2.1041	12.0336	0.99631
CEEMD-ST-ResNet-CNN-LSTM	1.5947	0.040587	1.1793	2.5596	0.99922

Table 19. The performance comparison of different models (during validation).

Model	RMSE	MAPE	MAE	MSE	R^2
LSTM	29.0921	846.3509	26.0169	846.3509	-3.906
GRU	33.6277	0.22907	29.3551	1130.8193	-5.555
SVM	17.0298	0.12037	15.1589	290.0124	-0.68111
CNN	25.413	0.38269	11.8285	645.822	-2.7436
CNN-LSTM	42.0043	0.30413	38.5155	1764.3646	-9.2275
CEEMD-ST-ResNet-CNN-LSTM	12.9028	0.089886	10.9997	166.4817	0.034958

Table 20. The performance comparison of different models (during training).

Model	RMSE	MAPE	MAE	MSE	R^2
LSTM	30.0973	0.75199	26.2288	905.8466	-0.31487
GRU	30.2831	0.74778	26.2885	917.0686	-0.33116
SVM	23.2908	0.48605	20.0899	542.4618	0.2126
CNN	24.6474	0.52245	18.7996	607.4943	0.1182
CNN-LSTM	21.5703	0.49391	18.5196	465.2761	0.32464
CEEMD-ST-ResNet-CNN-LSTM	26.1248	0.64509	22.4533	682.5035	0.0093219

4.5. Comparison experiment

Comparative experiments are conducted in this study to assess the impact of CEEMD on prediction performance relative to other modal decomposition methods. The predicted curves are shown in Figure 5.

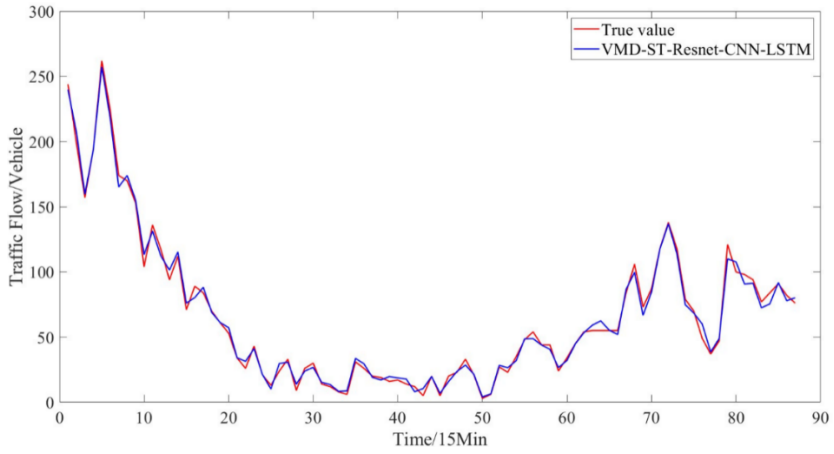

(a)

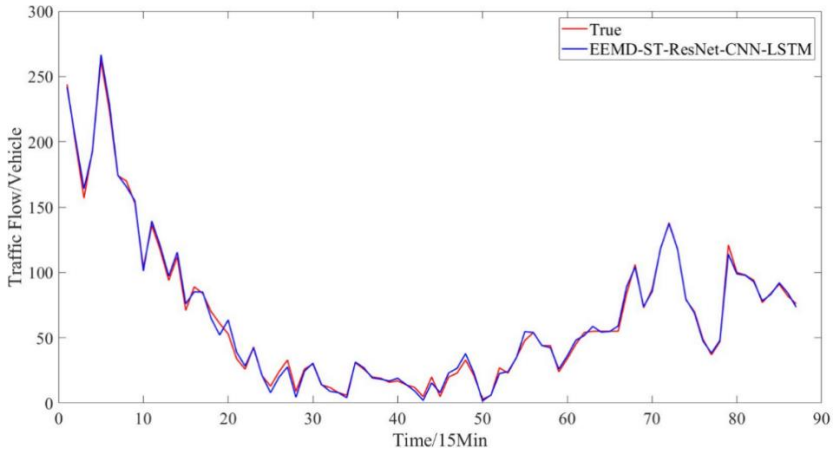

(b)

continued on next page

Figure 5. The comparison chart of predictions. (a) Prediction of VMD-ST-ResNet-CNN-LSTM; (b) Prediction of EEMD-ST-ResNet-CNN-LSTM; (c) Prediction of CEEMDAN-ST-ResNet-CNN-LSTM; (d) Prediction of CEEMD-ST-ResNet-CNN-LSTM.

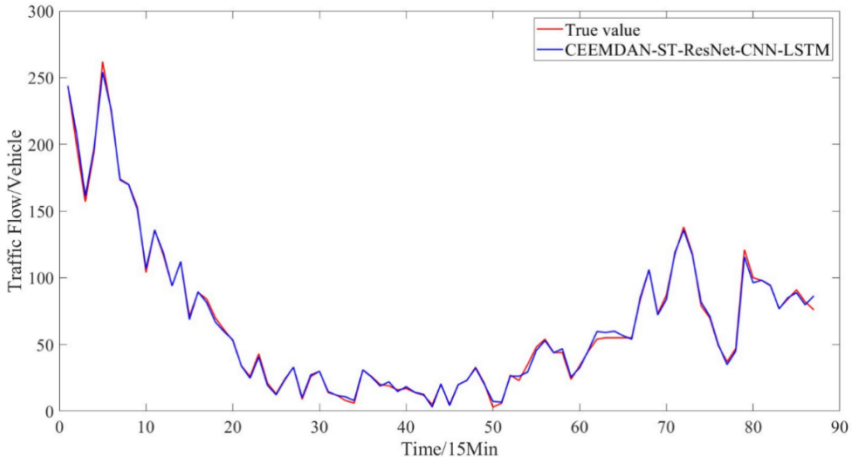

(c)

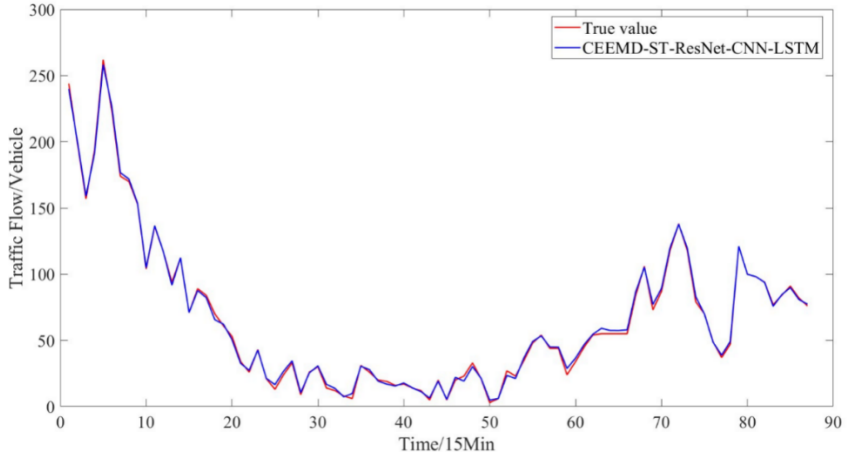

(d)

Figure 5. The comparison chart of predictions. (a) Prediction of VMD-ST-ResNet-CNN-LSTM; (b) Prediction of EEMD-ST-ResNet-CNN-LSTM; (c) Prediction of CEEMDAN-ST-ResNet-CNN-LSTM; (d) Prediction of CEEMD-ST-ResNet-CNN-LSTM.

VMD-ST-ResNet-CNN-LSTM: The variational mode decomposition decomposes a non-stationary signal into modal functions, each representing a vibration mode in a frequency range. The maximum number of modal decompositions is six, and the number of deep spatio-temporal residual filters is 60.

EEMD-ST-ResNet-CNN-LSTM: After adding various Gaussian white noise components in the original signal and decomposing it multiple times, ensemble empirical mode decomposition mitigates modal aliasing and pseudo-modal generation. This approach enhances the processing of non-linear and non-smooth signals. The max number of modes is seven, and the number of deep spatio-temporal residual filters is 68.

CEEMDAN-ST-ResNet-CNN-LSTM: This model completes ensemble empirical mode decomposition with adaptive noise effectively and is able to handle non-linear and non-smooth signals. It uses noise rounds and integration to improve the robustness towards noise and modal aliasing. The maximum number of modes is limited to seven, while the number of deep space-time residual filters is set at 80.

CEEMD-ST-ResNet-CNN-LSTM: The proposed model utilizes CEEMD to enhance decomposition accuracy and stability. It achieves this by adaptively decomposing the signal into

multiple IMFs and averaging over multiple decompositions. This approach offers wide applicability and improved performance. The max number of modes is six, and the number of deep spatio-temporal residual filters is 58.

Based on Tables 21–23, it is evident that the CEEMD-ST-ResNet-CNN-LSTM model proposed in this study achieves significant improvements as compared to other optimal modal decomposition models. Specifically, it reduces the RMSE by 29.21%, the MAPE by 25.55%, the MAE by 21.89%, the MSE by 49.56%, and the coefficient of determination by up to 99.92%. These results indicate that the selected CEEMD outperforms other decomposition models.

Table 21. The performance analysis of different models (during training).

Model	RMSE	MAPE	MAE	MSE	R^2
VMD-ST-ResNet-CNN-LSTM	4.1849	0.099607	3.2482	17.5132	0.99462
EEMD-ST-ResNet-CNN-LSTM	3.2243	0.085606	2.4755	10.396	0.99681
CEEMDAN-ST-ResNet-CNN-LSTM	2.2528	0.054516	1.5098	5.0749	0.99844
CEEMD-ST-ResNet-CNN-LSTM	1.5947	0.040587	1.1793	2.5596	0.99922

Table 22. The performance analysis of different models (during validation).

Model	RMSE	MAPE	MAE	MSE	R^2
VMD-ST-ResNet-CNN-LSTM	8.819	0.060692	7.5414	77.775	0.54916
EEMD-ST-ResNet-CNN-LSTM	22.7674	0.15374	19.7706	518.3552	-2.0047
CEEMDAN-ST-ResNet-CNN-LSTM	12.8946	0.084237	10.4133	166.2715	0.036176
CEEMD-ST-ResNet-CNN-LSTM	12.9028	0.089886	10.9997	166.4817	0.034958

Table 23. The performance analysis of different models (during test).

Model	RMSE	MAPE	MAE	MSE	R^2
VMD-ST-ResNet-CNN-LSTM	34.7092	0.77	30.9936	1204.7275	-0.7487
EEMD-ST-ResNet-CNN-LSTM	26.4244	0.65379	24.1879	698.2508	-0.013536
CEEMDAN-ST-ResNet-CNN-LSTM	24.5746	0.53628	21.5213	603.9089	0.1234
CEEMD-ST-ResNet-CNN-LSTM	26.1248	0.64509	22.4533	682.5035	0.0093219

The results show that the CEEMD-ST-ResNet-CNN-LSTM model proposed in this study improves all the indexes as compared to other models. This suggests that the model effectively reduces the impact of external factors and non-linear sequence noise on traffic flow data. As a result, the model provides more accurate judgments with wider applicability. The proposed method has reference value in the field of intelligent transportation systems.

5. Conclusions

In this study, a hybrid model is proposed for short-term traffic flow prediction using empirical modal decomposition of complementary ensembles. The proposed model fully extracts the spatio-temporal features, thus reducing the impact of external factors like weather and holidays. Meanwhile, the utilization of complementary ensemble empirical modal decomposition effectively reduces the

impact of non-linear sequence noise in the traffic flow sequence, thereby enhancing the accuracy and practicality of the model. The advantages are as follows:

1) The application of spatio-temporal residual connections effectively addresses the problems caused by vanishing and exploding gradients and improves the model's generalization ability and cross-layer stability.

2) The spatio-temporal attention mechanism effectively learns important regions and key information in spatio-temporal data. It also learns weights for different spatio-temporal characteristics. This allows the model to focus more on the important spatio-temporal characteristics, improving prediction accuracy and applicability.

3) Furthermore, the complementary ensemble empirical modal decomposition method dissects the traffic flow sequence into smoother components, effectively reducing the interference caused by the non-linear noise and improving the accuracy and efficiency of short-term traffic flow sequence prediction.

In this study, we apply a mixture of CEEMD, CNN and LSTM to the field of short-term traffic flow prediction, and introduce ST-ResNet to further improve the model prediction accuracy. In this study, CEEMD and ST-ResNet are applied to short-term traffic flow prediction together for the first time, which provides a new idea for short-term traffic flow prediction.

The results of the study demonstrate that all the prediction indexes of the proposed model have been improved with an accuracy of 99.92%, demonstrating high precision and applicability. It has some reference value in the field of short-term traffic flow prediction.

Future plans include incorporating additional external factors, such as traffic accidents, road construction, and traffic control, into the model. Additionally, a wider range of accurate and diverse data will be collected to reduce the model's reliance on input data. Data processing techniques will be optimized, and streaming data processing will be implemented to enhance the model's real-time and dynamic nature.

Use of AI tools declaration

The authors declare that they have not used Artificial Intelligence (AI) tools in the creation of this article.

Acknowledgments

This research was supported by the National Natural Science Foundation of China (Grant No. 51968063), Xizang Autonomous Region Science and Technology Plan " the open competition mechanism to select the best candidates" Project (Grant No. XZ202303ZY0005G), Academic development support program for young doctors of Tibet University (No. zdbs202212), Himalayan human activities and regional development collaborative innovation construction center project (No. 00060872) and Zangcai Yuzhi [2023] No.1 Central Support for the Construction of a Comprehensive Discipline Innovation Platform Project Supported by Local Departments and Regions-High Altitude Traffic Incident Assessment and Emergency Exercise Platform Construction Project.

Conflict of interest

The authors declare there is no conflict of interest.

References

1. H. Zheng, F. Lin, X. Feng, Y. Chen, A hybrid deep learning model with attention-based conv-LSTM networks for short-term traffic flow prediction, *IEEE Trans. Intell. Transp. Syst.*, **22** (2020), 6910–6920. https://doi.org/10.1109/TITS.2020.2997352
2. M. Wei, S. Zhang, T. Liu, B. Sun, The adjusted passenger transportation efficiency of nine airports in China with consideration of the impact of high-speed rail network development: A two-step DEA-OLS method, *J. Air. Transp. Manage.*, **109** (2023), 102395. https://doi.org/10.1016/j.jairtraman.2023.102395
3. M. Wei, S. Zhang, B. Sun, Comprehensive operating efficiency measurement of 28 Chinese airports using a two-stage DEA-Tobit method, *Electron. Res. Arch.*, **31** (2023), 1543–1555. https://doi.org/10.3934/era.2023078
4. X. Ma, J. Zhao, Y. Gong, X. Sun, Carrier sense multiple access with collision avoidance-aware connectivity quality of downlink broadcast in vehicular relay networks, *IET Microw. Antennas. Propag.*, **13** (2019), 1096–1103. https://doi.org/10.1049/iet-map.2018.6102
5. L. Li, Q. M. Zhang, J. H. Zhao, Y. W. Nie, Short-term traffic flow prediction method of different periods based on improved CNN-LSTM, *J. Appl. Sci.*, **39** (2021), 185–198. https://doi.org/10.3969/j.issn.0255-8297.2021.02.001
6. Y. Kamarianakis, P. Prastacos, Prediction traffic flow conditions in an urban network: Comparison of multivariate and univariate approaches, *Transp. Res. Rec.*, **1857** (2003), 74–84. https://doi.org/10.3141/1857-09
7. M. Castro-Neto, Y. S. Jeong, M. K. Jeong, L. D. Han, Online-SVR for short-term traffic flow prediction under typical and atypical traffic conditions, *Expert. Syst. Appl.*, **36** (2009), 6164–6173. https://doi.org/10.1016/j.eswa.2008.07.069
8. Y. Lv, Y. Duan, W. Kang, Z. Li, F. Y. Wang, Traffic flow prediction with big data: A deep learning approach, *IEEE Trans. Intell. Transp. Syst.*, **16** (2014), 865–873. https://doi.org/10.1109/TITS.2014.2345663
9. J. Zhao, Y. Nie, S. Ni, X. Sun, Traffic data imputation and prediction: An efficient realization of deep learning, *IEEE Access*, **8** (2020), 46713–46722. https://doi.org/10.1109/ACCESS.2020.2978530
10. W. Lu, Z. Yi, W. Liu, Y. Gu, Y. Rui, B. Ran, Efficient deep learning based method for multi-lane speed prediction: a case study in Beijing, *IET Intell. Transp. Syst.*, **14** (2020), 2073–2082. https://doi.org/10.1049/iet-its.2020.0410
11. R. Liu, Y. Liu, J. Gu, Improved AdaNet based on adaptive learning rate optimization, *J. Comput. Appl.*, **40** (2020), 2804. https://doi.org/10.11772/j.issn.1001-9081.2020020237
12. L. I. U. Yi-cheng, L. I. Zhi-peng, L. V. Chun-pu, Z. H. A. N. G. Tao, L. I. U. Yan, Network-wide traffic flow prediction research based on DTW algorithm spatial-temporal graph convolution, *J. Transp. Syst. Eng. Inf. Technol.*, **2** (2022), 147. https://doi.org/10.16097/j.cnki.1009-6744.2022.03.017
13. S. Halyal, R. H. Mulangi, M. M. Harsha, prediction public transit passenger demand: With neural networks using APC data, *Case Stud. Transp. Policy*, **10** (2022), 965–975. https://doi.org/10.1016/j.cstp.2022.03.011
14. Y. Feng, J. Hao, X. Hao, J. Li, Forecasting short-term tourism demand with a decomposition-ensemble strategy, *Proc. Comput. Sci.*, **199** (2022), 879–884. https://doi.org/10.1016/j.procs.2022.01.110
15. Y. Bai, Z. Sun, B. Zeng, J. Deng, C. Li, A multi-pattern deep fusion model for short-term bus passenger flow prediction, *Appl. Soft. Comput.*, **58** (2017), 669–680. https://doi.org/10.1016/j.asoc.2017.05.011

16. S. I. Alzahrani, I. A. Aljamaan, E. A. Al-Fakih, Forecasting the spread of the COVID-19 pandemic in Saudi Arabia using ARIMA prediction model under current public health interventions, *J. Infect. Public Health*, **13** (2020), 914–919. https://doi.org/10.1016/j.jiph.2020.06.001
17. W. Huang, G. Song, H. Hong, K. Xie, Deep architecture for traffic flow prediction: deep belief networks with multitask learning, *IEEE Trans. Intell. Transp. Syst.*, **15** (2014), 2191–2201. https://doi.org/10.1109/TITS.2014.2311123
18. Y. U. A. N. Hua, C. H. E. N. Zehao, Short-term traffic flow prediction based on temporal convolutional networks, *Sch. Comput. Sci. Eng., S. China Univ. Technol.*, **48** (2020), 107–113. https://doi.org/10.12141/j.issn.1000-565X.190276
19. X. Ma, Z. Tao, Y. Wang, H. Yu, Y. Wang, Long short-term memory neural network for traffic speed prediction using remote microwave sensor data, *Transp. Res. Part C: Emerg. Technol.*, **54** (2015), 187–197. https://doi.org/10.1016/j.trc.2015.03.014
20. B. Hussain, M. K. Afzal, S. Ahmad, A. M. Mostafa, Intelligent traffic flow prediction using optimized GRU model, *IEEE Access*, **9** (2021), 100736–100746. https://doi.org/10.1049/iet-its.2018.5593
21. W. Jiang, J. Luo, Graph neural network for traffic forecasting: A survey, *Expert. Syst. Appl.*, **207** (2022), 117921. https://doi.org/10.48550/arXiv.2101.11174
22. Y. Li, S. Chai, Z. Ma, G. Wang, A hybrid deep learning framework for long-term traffic flow prediction, *IEEE Access*, **9** (2021), 11264–11271. https://doi.org/10.1109/ACCESS.2021.3050836
23. X. Yang, Q. Xue, X. Yang, H. Yin, Y. Qu, X. Li, et al., A novel prediction model for the inbound passenger flow of urban rail transit, *Inf. Sci.*, **566** (2021), 347–363. https://doi.org/10.1016/j.ins.2021.02.036
24. J. Zhang, F. Chen, Q. Shen, Cluster-based LSTM network for short-term passenger flow prediction in urban rail transit, *IEEE Access*, **7** (2019), 147653–147671. https://doi.org/10.1109/ACCESS.2019.2941987
25. X. Ma, Z. Dai, Z. He, J. Ma, Y. Wang, Y. Wang, Learning traffic as images: A deep convolutional neural network for large-scale transportation network speed prediction, *Sensors*, **17** (2017), 818. https://doi.org/10.3390/s17040818
26. J. Zhang, Y. Zheng, D. Qi, R. Li, X. Yi, T. Li, Predicting citywide crowd flows using deep spatio-temporal residual networks, *Artif. Intell.*, **259** (2018), 147–166. https://doi.org/10.1016/j.artint.2018.03.002
27. Z. Wu, N. E. Huang, Ensemble empirical mode decomposition: a noise-assisted data analysis method, *Adv. Adapt. Data Anal.*, **1** (2009), 1–41. https://doi.org/10.1142/S1793536909000047
28. J. R. Yeh, J. S. Shieh, N. E. Huang, Complementary ensemble empirical mode decomposition: A novel noise enhanced data analysis method, *Adv. Adapt. Data Anal.*, **2** (2010), 135–156. https://doi.org/10.1142/S1793536910000422
29. P. Lou, Z. Wu, J. Hu, Q. Liu, Q Wei, Attention-based gated recurrent graph convolutional network for short-term traffic flow prediction, *J. Math.*, **2023** (2023). https://doi.org/10.1155/2023/6933344
30. B. Li, Q. Yang, J. Chen, D. Yu, D. Wang, F. Wan, A dynamic spatio-temporal deep learning model for lane-level traffic prediction, *J. Adv. Transp.*, **2023** (2023). https://doi.org/10.1155/2023/3208535
31. Z. Yang, C. Wang, Short-term traffic flow prediction based on AST-MTL-CNN-GRU, *IET Intell. Transp. Syst.*, 2023. https://doi.org/10.1049/itr2.12400
32. K. Zhao, D. Guo, M. Sun, C. Zhao, H. Shuai, Short-term traffic flow prediction based on VMD and IDBO-LSTM, *IEEE Access*, 2023. https://doi.org/10.1109/ACCESS.2023.3312711

33. W. Zhao, Y. Yang, Z. Lu, Interval short-term traffic flow prediction method based on CEEMDAN-SE nosie reduction and LSTM optimized by GWO, *Wireless Commun. Mobile Comput.*, **2022** (2022). https://doi.org/10.1155/2022/5257353
34. X. Jiang, A combined monthly precipitation prediction method based on CEEMD and improved LSTM, *Plos One*, **18** (2023), e0288211. https://doi.org/10.1371/journal.pone.0288211
35. X. Chen, S. Wu, C. Shi, Y. Huang, Y. Yang, R. Ke, et al., Sensing data supported traffic flow prediction via denoising schemes and ANN: A comparison, *IEEE Sens. J.*, **20** (2020), 14317–14328. https://doi.org/10.1109/JSEN.2020.3007809
36. J. R. Yeh, J. S. Shieh, N. E. Huang, Complementary ensemble empirical mode decomposition: A novel noise enhanced data analysis method, *Adv. Adapt. Data Anal.*, **2** (2010), 135–156. https://doi.org/10.1142/S1793536910000422
37. Abdeljaber, O. Avci, S. Kiranyaz, M. Gabbouj, D. J. Inman, Real-time vibration-based structural damage detection using one-dimensional convolutional neural networks, *J. Sound Vib.*, **388** (2017), 154–170. https://doi.org/10.1016/j.jsv.2016.10.043
38. Y. J. Li, J. J. Huang, H. Y. Huang, N. Huang, Study of emotion recognition based on fusion multi-modal bio-signal with SAE and LSTM recurrent neural network, *J. Commun.*, **38** (2017), 109–120. https://doi.org/10.11959/j.issn.1000-436x.2017294
39. J. Fan, Q. Li, J. Hou, X. Feng, H. Karimian, S. Lin, A spatiotemporal prediction framework for air pollution based on deep RNN, *ISPRS Ann. Photogramm. Remote Sens. Spat. Inf. Sci.*, **4** (2017), 15–22. https://doi.org/10.5194/isprs-annals-IV-4-W2-15-2017
40. Y. A. N. G. Yi-Yue, F. U. Qian, W. Qian, A prediction model for time series based on deep recurrent neural network, *Comput. Technol. Dev.*, **27** (2017), 35–38. https://doi.org/10.3969/j.issn.1673-629X.2017.03.007
41. R. Shi, L. Du, Multi-section traffic flow prediction based on MLR-LSTM neural network, *Sensors*, **22** (2022), 7517. https://doi.org/10.3390/s22197517
42. H. Zeng, Z. Peng, X. Huang, Y. Yang, R. Hu, Deep spatio-temporal neural network based on interactive attention for traffic flow prediction, *Appl. Intell.*, (2022), 1–12. https://doi.org/10.1007/s10489-021-02879-1
43. J. Yang, X. Dong, H. Yang, X. Han, Y. Wang, J. Chen, Prediction of inbound and outbound passenger flow in urban rail transit based on spatio-temporal attention residual network, *Appl. Sci.*, **13** (2023), 10266. https://doi.org/10.3390/app131810266
44. J. Zhou, H. Chang, X. Cheng, X. Zhao, A multiscale and high-precision LSTM-GASVR short-term traffic flow prediction model, *Complexity*, **2020** (2020), 1–17. https://doi.org/10.1155/2020/1434080
45. S. Xue, C. Shao, S. Wang, Y. Zhuang, Deep learning with bidirectional long short-term memory for traffic flow prediction, *J. Phys. Conf. Ser.*, **1972** (2021), 012098. https://doi.org/10.1088/1742-6596/1972/1/012098
46. L. Zhang, Q. Zhang, W. Yang, N. Wei, D. Dong, An improved k-nearest neighbor model for short-term traffic flow prediction, *Procedia Soc. Behav. Sci.*, **96** (2013), 653–662. https://doi.org/10.1016/j.sbspro.2013.08.076